Erschienen in: Soft Matter ; 7 (2011), 4. - S. 1352-1357
https://dx.doi.org/10.1039/C0SM00486C

Phase behavior of colloidal monolayers in quasiperiodic light fields†

Jules Mikhael,[a] Günter Gera,[a] Thomas Bohlein[ab] and Clemens Bechinger*[ab]

We experimentally investigate the phase behavior of a dense two dimensional system of interacting colloidal particles subjected to a decagonal quasiperiodic potential landscape created by the interference of five laser beams. Upon increasing the intensity I_0 of the laser field, we observe the initial triangular crystal to change into a quasicrystal *via* a two step process. To characterize this transition, we apply an algorithm that describes the resulting structures in terms of a polygonal tiling comprised of triangular, square and pentagonal tiles. First, square tiles develop at the expense of triangular tiles and assemble into bands. Only at higher laser intensities, pentagonal tiles, which reflect the decagonal quasiperiodic ordering, occur. For certain particle densities, an Archimedean like tiling occurs where the bands of square extend across the entire system. We demonstrate how the alignment of these bands can be related to phasonic strain fields in the laser pattern.

Introduction

Since the discovery of the first quasicrystal in the early 1980s,[1,2] it is now established that materials with long range order but without translational symmetry exist. While first examples of such structures were mainly observed in complex metallic alloys,[3,4] in the meantime also quasicrystals in soft matter systems have been found.[5–7] Quasicrystals (QCs) behave rather unusual compared to periodic crystals regarding mechanical, electrical, optical and other properties.[8–10] Accordingly, QCs are believed to have a large potential for technological applications such as surface coatings, thermal barriers, catalysts or photonic devices.[8] Still, it is unclear whether the origin of these charac teristics is due to the chemical or the structural complexity inherent to QCs. Therefore, recent research aims to impose quasiperiodic order (and perhaps also typical quasiperiodic properties) to single element layers by adsorbing them onto QC surfaces. Indeed, thin films of lead atoms adopt the quasiperiodic structure of the underlying substrate (pseudomorphic growth) when adsorbed onto such surfaces.[11–13] But there exist also other materials where the competition between the interactions within the adsorbate and those with the substrate lead to even more complex structures.[14,15] For a systematic investigation of the phase behavior of interacting adsorbates on quasiperiodic surfaces, it would be ideal, if the relevant interactions and length scales could be independently adjusted. This, however, is difficult to achieve, since *e.g.* adsorbate adsorbate interactions are not independent of the corresponding interaction with the substrate.

It has been recently demonstrated, that colloidal monolayers interacting with quasiperiodic light fields comprise an excellent model system for understanding their structural properties.[16–18] Since in such experiments all the aforementioned parameters can be varied independently over a large range, this allows for a systematic investigation of the phase behavior of interacting monolayers on quasiperiodic surfaces. Here, we report an experimental study of the phase transition of a two dimensional (2D) colloidal system from a triangular crystal to a decagonal quasicrystal when subjected to a quasiperiodic laser field.[16,18] We analyze this transition by means of a tiling algorithm which allows to describe the colloidal structure by v fold polygons. Our results demonstrate that only at rather high laser fields pentag onal tiles being the dominant motive in the underlying deca gonal laser pattern are observed. In addition, we show how phasonic strain fields within the quasiperiodic light field influence the ordering of the colloidal structures.

Experimental methods and data analysis

In our experiments, we use highly charged micrometre sized spherical polystyrene particles with radius $R = 1.45$ μm and a polydispersity of about 4% which are suspended in water. Due to surfaces charges, the particles interact *via* a repulsive screened Coulomb potential which is in units of the thermal energy k_BT

$$u(r)/k_BT = \left(\frac{Z_{\text{eff}}\exp[\kappa R]}{1+\kappa R}\right)^2 \lambda_B \frac{\exp[\quad \kappa r]}{r}$$

where r is the center center particle distance, Z_{eff} the effective colloidal charge, κ^{-1} the Debye screening length set by the amount of ions in the suspension and λ_B the Bjerrum length (0.72 nm in water). For our particles Z_{eff} has been determined to about 140,000.[19] This value is also in good agreement with direct pair interaction measurements of other authors.[20] To enhance the electrostatic particle interaction, we reduce the number of ions in the suspension by adding deionized water to the suspension, centrifuging the sample, and removing excess solvent. Finally, the suspension is inserted into the sample cell which is comprised of a flat cuvette of silica plates with a spacing of 200 μm. After sealing the two inlets of the sample cell, this leads to a Debye screening length of about $\kappa^{-1} \approx 160$ nm which remains stable over several hours.[16] Due to the large value of the prefactor in u(r), the range of the pair potential of colloidal particles, *i.e.* the distance

[a]2. Physikalisches Institut, Universitat Stuttgart, Pfaffenwaldring 57, 70569 Stuttgart, Germany. E mail: c.bechinger@physik.uni stuttgart.de; Fax: +49 71168565285; Tel: +49 7168565217
[b]Max Planck Institut fur Metallforschung, Heisenbergstraße 3, 70569 Stuttgart, Germany

† This paper is part of a *Soft Matter* themed issue dedicated to the International Soft Matter Conference 2010.

where the electrostatic interaction energy is on the order of k_BT largely exceeds the Debye screening length.

Owing to the counterplay of gravitational forces and electro static repulsion with the negatively charges silica surfaces, the particles are localized above the bottom of the sample cell at a distance estimated to be higher than 500 nm. In particular at high particle densities, electrostatic particle interactions lead to large vertical particle fluctuations or even buckling[21] of the monolayer which would disturb our measurements. To enforce a 2D colloidal system we therefore suppressed such effects by a vertically incident laser beam ($\lambda = 514$ nm) which exerts an optical pressure on the colloids towards the lower plate of the sample cell.

Quasiperiodic potentials are created by interfering five laser beams (Fig. 1a).[22] The single beam of a linearly polarized frequency doubled Nd:YAG laser ($\lambda = 532$ nm) is divided with a multi beam interferometer into five parallel beams of identical polarization and intensity. After the beams pass a convex lens, they converge and overlap inside the sample cell where they form an interference pattern with decagonal quasiperiodic symmetry[23]

$$I(r) = I_0 \left| \sum_{j}^{5} \exp(iG_j r) \right|^2$$

Here, G_1 to G_5 correspond to the wavevectors of the incident partial beams and I_0 to the total laser intensity. Fig. 1b shows the calculated light intensity distribution in the sample plane, which displays maxima arranged in pentagons of different sizes and orientations. Their side lengths are related by the golden ratio $\tau = (1+\sqrt{5})/2 = L/S$ where L and S are the characteristic length scales of the pattern which can be experimentally adjusted between ~4 and 15 μm by the angle of incidence under which the laser beams converge. Due to optical gradient forces, the inter ference pattern can be regarded as a substrate potential for the colloidal particles where the substrate strength can be adjusted by the laser intensity I_0.

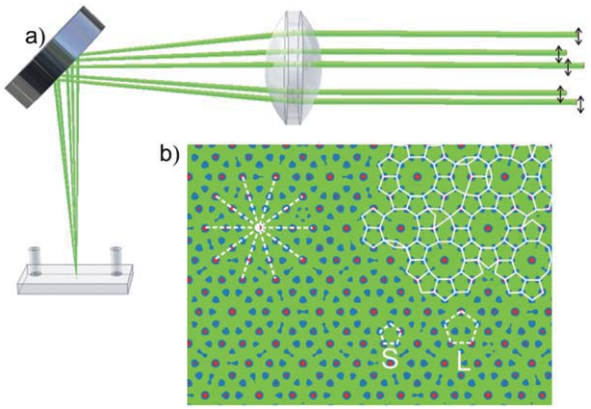

Fig. 1 (a) Sketch of the experimental realization of a decagonal inter ference pattern. Five linearly polarized (black arrows) laser beams form a regular pentagon and are focused into a thin sample cell. (b) Numeri cally calculated intensity distribution of the pattern which acts as a substrate potential for the colloids due to optical forces. The solid white lines show the tiling into polygons using the algorithm described in Fig. 2. The pattern displays a decagonal symmetry and the predominating motives are pentagons with different sizes (S, L) with a side length related by the golden ratio τ (indicated in dashed white). The white dashed lines correspond to the directions of the incident laser beams. The colour coding of the intensity field ranges from green to red and reflects the potential well depth variation.

Particle positions are registered with digital video microscopy with a sampling rate of 1 Hz and a spatial resolution of 150 nm. From the obtained data, we calculate *e.g.* the 2D structure factor $S(q_x,q_y)$ given by

$$S(q_x, q_y) = \frac{1}{N} \sum_{j,k}^{N} \exp(iqr_{jk})$$

where q is the reciprocal wave vector, N the number of colloidal particles, and r_{jk} the center to center distance between particle j and k.

For the detection of the local particle configurations, *i.e.* geometrical defects, we applied an algorithm, which divides the colloidal structure into elementary polygonal tiles.[24] As illustrated in Fig. 2, the algorithm is based on the Delaunay triangulation (DT) (Fig. 2a), which creates a network of bonds connecting each particle to its next neighbors. To identify stable local particle configurations, we first remove bonds which are unstable against particle fluctuations. This is achieved by first constructing the Voronoi tessellation, *i.e.* the dual construction of the Delaunay triangulation, which divides the plane into cells where each edge corresponds to a bond in Delaunay triangula tion (see Fig. 2b). In contrast to the long edges which are very stable against small particle fluctuations, this is not true for the short edges (red lines in Fig. 2c) which are often found to

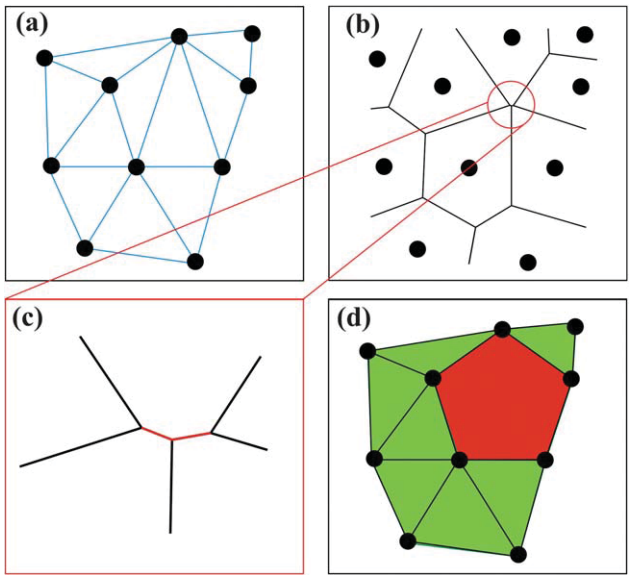

Fig. 2 Illustrative example of the tiling algorithm procedures. (a) Delaunay triangulation of 10 random particles (black dots) identifying next neighbour bonds (blue lines). The tiling contains only triangular tiles. (b) Voronoi tessellation of the particle configuration in (a) dividing the plane into adjacent cells (black lines). (c) Zoom on the short edges (red lines) that occur in the Voronoi tessellation in (b). These edges are not stable against particle fluctuations and their corresponding bonds in the Delaunay triangulation are removed. (d) Resulting tiling after removal of the bonds showing stable triangular (green) and pentagonal (red) tiles.

disappear from frame to frame. When the bonds in the Delaunay triangulation which are responsible for these short edges are removed, this finally generates a tiling which is rather stable against thermal fluctuations. It is important to realize, that this procedure generates also higher order v fold polygonal tiles, such as 4 fold (square) or 5 fold (pentagonal) tiles (Fig. 2d). For a quantitative analysis, the density of the v folded tiles (ρ_v) is calculated. It should be noted that this tiling algorithm is not identical to *e.g.* Penrose tilings[25] since our algorithm does not consider matching rules between the tiles.

Results and discussion

Fig. 3 shows the structural change of a 2D colloidal monolayer subjected to a quasiperiodic interference pattern of increasing laser intensity. Here, the particle density is adjusted to $\phi = 0.032$ μm ^{2} corresponding to a mean particle distance $a_P = 5.97$ μm. Consid ering the values for the characteristic length scales $L = 9.3$ μm and S = 5.6 μm of the laser pattern, the number of relevant potential wells provided by the light field is about 25% smaller than the number of particles. Since the range of the colloidal pair potential is larger than a_P, the phase behavior is the result of a competition between electrostatic and optical forces which favor a triangular and decagonal symmetry, respectively.

At small laser intensities $I_0 < 2.0$ μWμm ^{2} (data not shown), electrostatic interactions prevail and a 2D crystal forms. Upon further increasing the laser field to $I_0 = 2.45$ μWμm ^{2}, in addition to triangular tiles (green) we find also squares (blue), pentagons (red) or even higher order polygons (white) (Fig. 3a). The cor responding 2D structure factor (Fig. 3b) exhibits 6 fold coordi nated peaks and thus confirms the despite the occurrence of non triangular tiles rather periodic order in the structure. When further increasing the interaction of the monolayer with the quasiperiodic light field ($I_0 = 3.15$ μWμm ^{2}) the density of triangular tiles decreases as seen in Fig. 3c. This is not surprising, because triangular tiles are not present in a decagonal light pattern (see Fig. 1b) and should therefore not occur in the colloidal monolayer. Interestingly, however, the decrease of triangular tiles is mainly in favor of an increase of square tiles (the fraction of pentagonal tiles remains almost constant). Since square tiles do neither occur in the colloidal periodic crystal and in the quasiperiodic light pattern, they must be a result of the competition of the mutual colloidal interaction and the optical forces. Clearly, the square tiles are not randomly distributed but form short, densely packed bands which are aligned along the crystal directions. The corresponding structure factor (Fig. 3d) still exhibits a pronounced 6 fold rotational symmetry. In addi tion, however, a weak precursor of colloidal quasiperiodic order appears as indicated by the formation of 10 fold coordinated spots (red arrows).

At $I_0 = 4.55$ μWμm ^{2} the number of triangular tiles decreases further and a strong increase of pentagonal tiles is observed (almost one order of magnitude). At the same time, the number of square tiles only increases by about 50% (Fig. 3e). The pentagonal tiles are not homogeneously distributed but assemble in clusters similar to those found in the tiling of the quasiperiodic laser field (Fig. 1b). Obviously, at this laser intensity, the colloidal structure is dominated by the interaction with the light field and the colloids thus follow the geometry of the decagonal interference pattern. This is also seen by the formation of the 10 fold symmetry in the structure factor (Fig. 3f).

Fig. 3g, finally shows the tiling for the maximum available laser intensity, $I_0 = 6.47$ μWμm ^{2}. The number of pentagons increases here by a factor of 2.6 while the number of squares increases only by a factor of 1.2. The diffraction pattern in Fig. 3h shows a higher order of quasicrystallinity indicating that

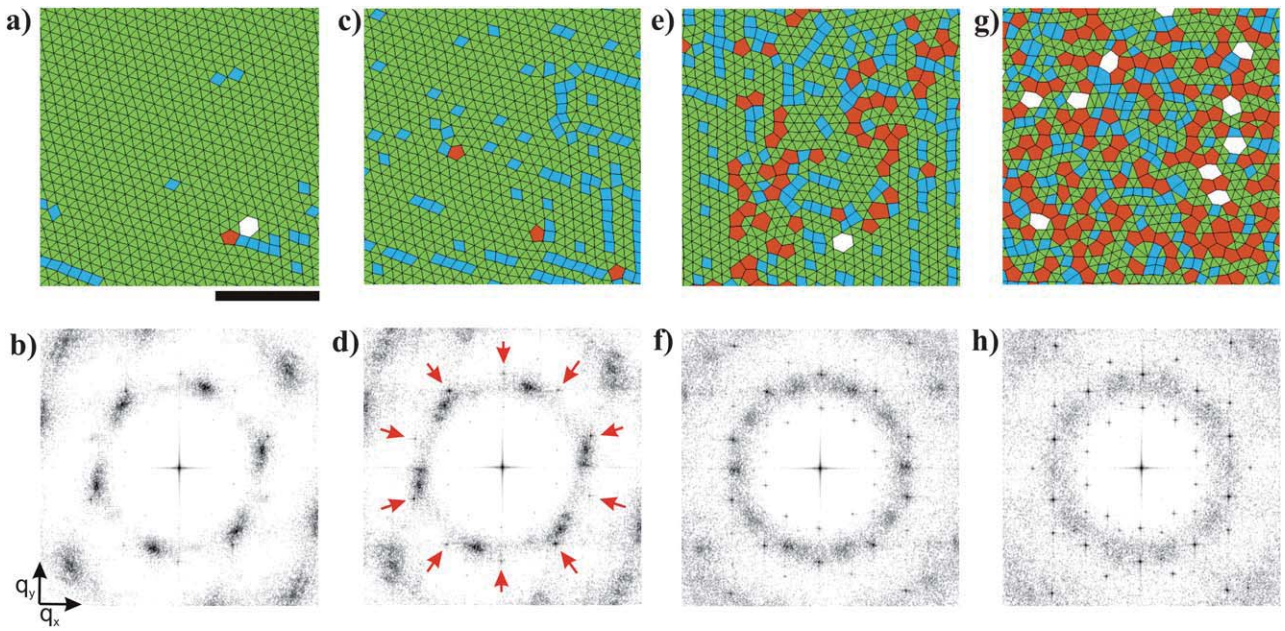

Fig. 3 Polygonal tiling and structure factor of a colloidal monolayer exposed to a decagonal substrate potential of increasing laser intensity I_0 in units of μW μm ^{2} (a) I_0 2.45, (c) 3.15, (e) 4.55, (g) 6.47. V folded polygons with v 3 are coloured in green, v 4 in blue, v 5 red, and higher order polygons in white. The scale bar corresponds to 50 μm. (b, d, f, h) $S(q_x,q_y)$ calculated for the data shown in (a, c, e, g). The red arrows in (d) point at the position where weak 10 fold peaks occur.

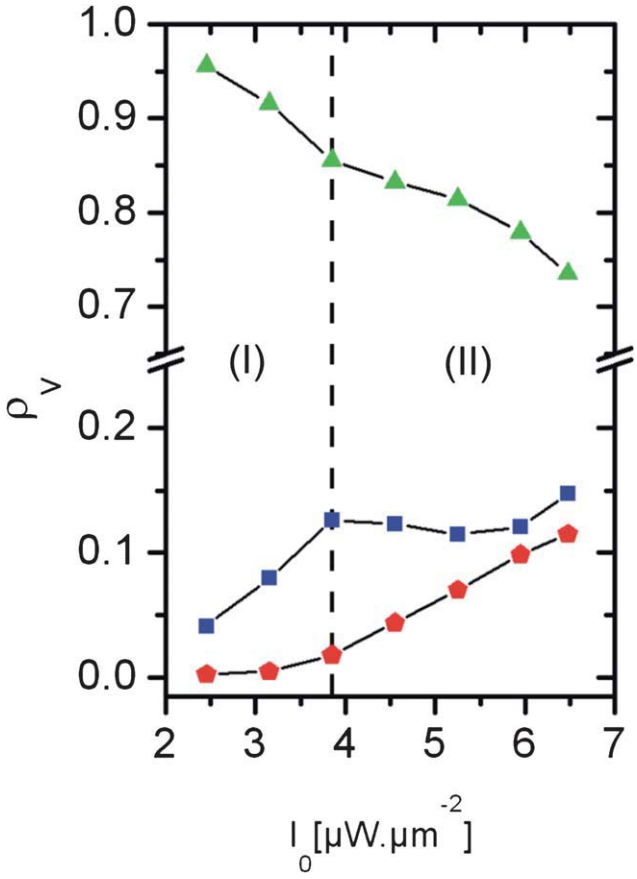

Fig. 4 Number density of v folded tiles as a function of I_0 as obtained from the data in Fig. 2. Triangular tiles (green), square tiles (blue) and pentagonal tiles (red). The vertical dashed line indicates the laser intensity where the square density saturates and the pentagonal tiles increase almost linearly.

a large number of the particles have adapted the symmetry of the underlying substrate.

In Fig. 4 we show how the fractions ρ_v of v fold polygons quantitatively change as a function of the interference pattern intensity. While ρ_3 almost linearly decreases with I_0, ρ_4 first increases until it satures at a value of about $\rho_4 = 12\%$. In contrast, the formation of pentagons is largely suppressed below a threshold value (dashed line) and then almost linearly increases. It has been already mentioned that the overall decrease of triangular tiles and increase of pentagonal tiles is in agreement with a gradual transition from a periodic triangular crystal to a decagonal quasicrystal. The occurrence of squares and their saturation at a rather constant fraction, however, is less obvious since they do no neither appear in tilings of the periodic colloidal crystal nor in the decagonal quasiperiodic laser lattice. The origin of square tiles will be discussed in detail further below.

Although the phase behavior a 2D triangular colloidal crystal on a quasiperiodic laser pattern is expected to strongly depend on the ratio of the characteristic length scales, *i.e.* a_P and S,L, the scenario discussed above is valid for a wide range of length scales. This has been also confirmed by recent Monte Carlo simulations which explored the phase behavior for different parameters.[26] However, for a narrow range of particle densities, a pronounced intermediate phase, a so called Archimedean like tiling, inter venes between the 2D triangular crystal and the quasicrystalline structure. In contrast to previous experiments,[16] where this phase has been experimentally observed, here we present a more detailed study, how it gradually develops from a triangular crystal.

Fig. 5 shows the behavior of a colloidal monolayer with a higher particle density $\phi = 0.040$ μm ^{2} (*i.e.* $a_P = 5.29$ μm). Under these conditions, an Archimedean like tiling phase should occur.[19] Similar to above, we observe a gradual decrease of triangular and a strong increase of square tiles with increasing

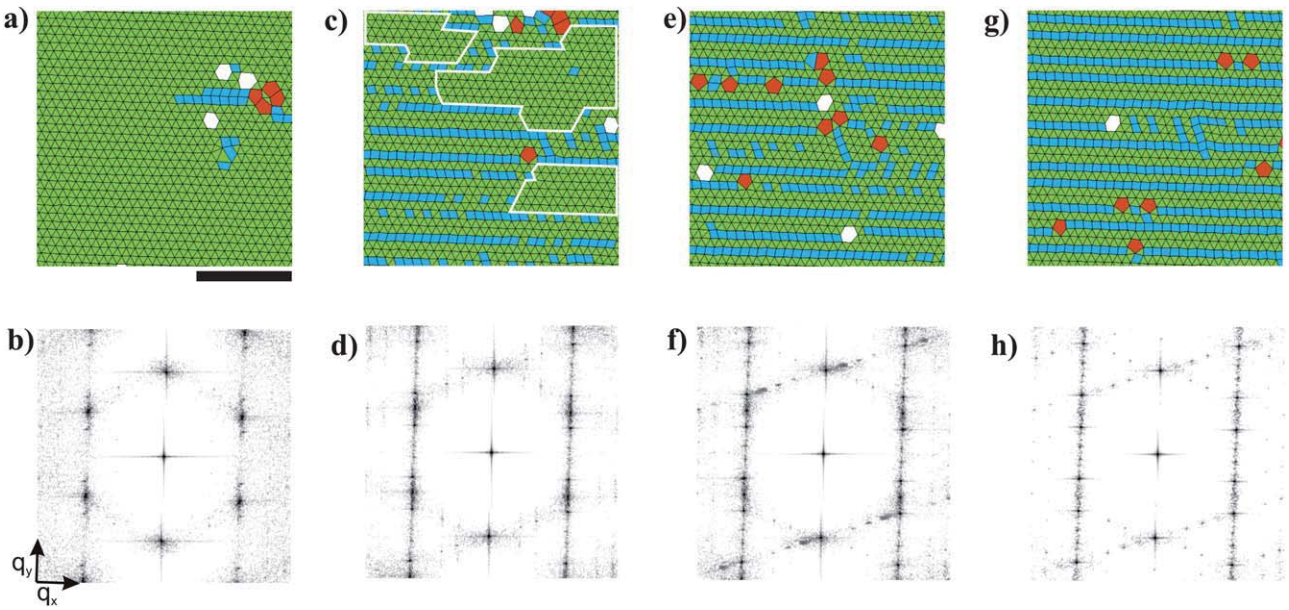

Fig. 5 Tiling and 2D structure factor of the colloidal monolayer. (a, c, e, g) Tiling of the crystalline phase for laser intensity I_0 1.5, 2.5, 3.0 and 4.0 μW μm ^{2}, respectively. The white lines in (c) highlight regions where a triangular periodic ordering is observed. The scale bar corresponds to 50 μm. (b, d, f, h) $S(q_x,q_y)$ calculated for the data shown in (a, c, e, g). The scale is exponential.

laser intensity (Fig. 6a,c,e,g). In contrast to Fig. 3, however, where short bands of square tiles were inhomogenously distrib uted across the monolayer, here they assemble as long bands extending almost across the entire system. As seen in Fig. 5e,g the increase of the laser intensity leads to an elongation in the length of the bands with square tiles, and an almost perfect ordering along the horizontal with some intrusions at an angle of 72°. The structure in Fig. 5g is well characterized by a tiling composed of squares and triangles arranged in bands. It should be realized that the sequence of triangular and square bands is not periodic but follows a Fibonacci sequence (with additionally triangular bands beeing inserted).[27] This ensures, that the colloidal system stays in registry with the underlying quasiperiodic potential even at large distances. The peaks in the corresponding $S(q_x,q_y)$ are periodically spaced along the q_x direction, whereas in the q_y direction their distance is close to the golden ratio (Fig. 5h). These features are characteristic for the Archimedean like tiling phase as recently found both in experiments[16] and computer simulation.[26] In contrast to previous studies, where the order of the phase transition could not be identified, the coexistence between the triangular and the Archimedean tiling phase as observed in Fig. 5c (white contour) strongly suggests a first order phase transition. Indeed, this is consistent with the arguments of Landau according to which first order transitions are generally expected when no continuous transition between the symmetries of the adjacent phases exists. Due to the smaller mean particle distance compared to Fig. 3, the strong electrostatic particle interaction prohibited a transition into the quasicrystalline phase within the range of laser intensities accessible in our experiments.

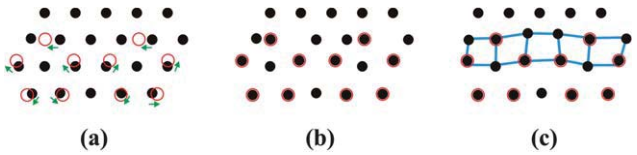

Fig. 6 Qualitative illustration of the formation of bands with square tiles. (a) Some particles (black dots) are attracted towards the nearest potential wells (red circles). The inhomogeneous particle distribution (b) is unfavourable due to the electrostatic repulsion, and the particles will maximize their distance to their nearest neighbours which eventually results in bands of square tiles (blue lines).

To qualitatively understand the origin of the square tiles, Fig. 6 schematically shows how a colloidal crystal (black bullets) becomes distorted by a quasiperiodic potential landscape. For simplicity, we only considered the deepest potential wells of the quasiperiodic pattern (red circles) which are arranged in penta gons (*cf.* Fig. 1b). The particle distances and the quasiperiodic pattern are drawn to scale and correspond to the situation in Fig. 5. Fig. 6a shows the situation at small laser intensities where the colloidal particles form a perfect 2D triangular crystal oriented along one of the five high symmetry direction of the decagonal QC lattice. With increasing I_0, a number of colloids is attracted towards the optical potential wells (indicated by green arrows). However, since the number of colloids exceeds that of deep laser potential wells, the remaining interstitial particles will rearrange to minimize the free energy of the system. As can be seen from Fig. 1b the quasiperiodic light field is rather uniform between the pentagonally arranged deep potential wells (red circles), therefore the forces acting on interstitial particles are dominated by the electrostatic repulsion. Accordingly, these particles favor an arrangement with uniform next neighbor

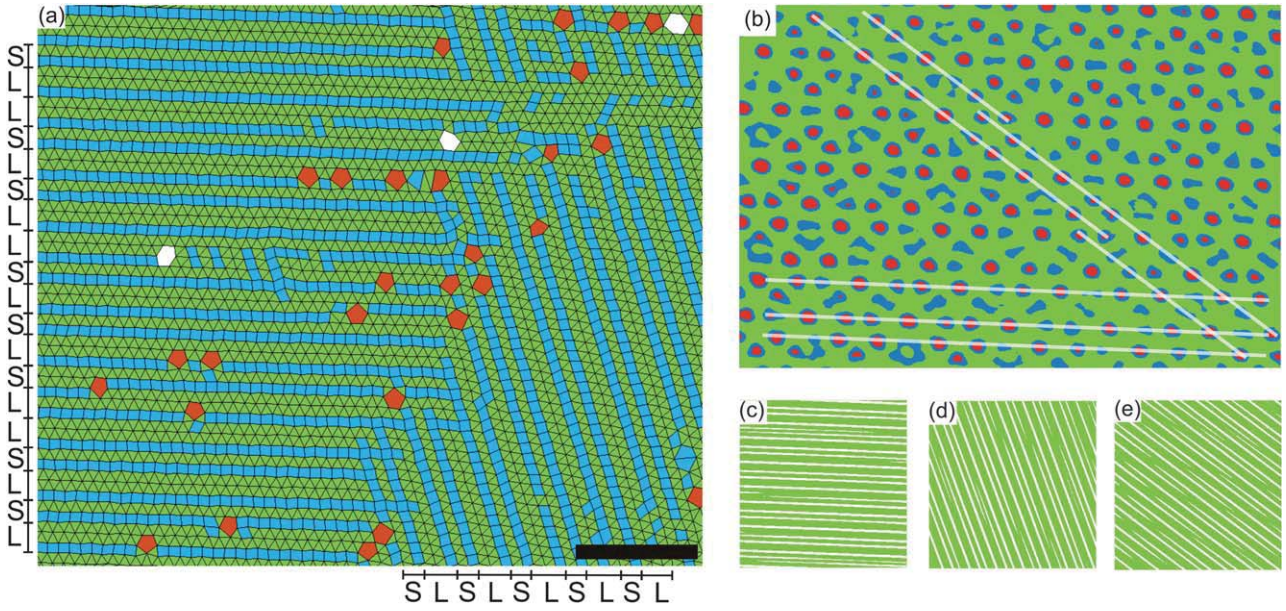

Fig. 7 (a) Tiling of the intermediate Archimedean like tiling with two differently aligned domains. The distance between the bands of square tiles in each domain follows a Fibonacci sequence with long (L) and short distances. The scale bar corresponds to 50 μm. (b) Section of the intensity distribution of the underlying interference pattern. The white lines which are broken along certain directions indicated the existence of phasonic strain fields which lead to jags along certain directions. (c,d,e) Images calculated by means of Fourier transformation showing the density of jags in the underlying pattern along three different orientations.

distance as shown in Fig. 6b,c. This eventually leads to the development of densely packed bands of (slightly distorted) square tiles (blue lines) which is in qualitative agreement with our experimental observations and also supported by recent Monte Carlo simulations.[19]

In principle, the direction of bands comprised of square tiles should correspond to one of the five orientations of the decagonal quasiperiodic laser lattice. In our experiments, however, we did not find an equal distribution of the bands along all five directions. A detailed analysis of the experimentally created quasiperiodic light pattern revealed, that this is related to the density of so called phasonic strain fields.[28] Phasons are similar to phonons collective excitations which are unique to quasicrystals.[29] For the quasiperiodic laser fields, the phasonic strain fields result in the occurrence of jags in characteristic lines which are infinitely extended in a strain free pattern. Experimentally, these jags occur when the tilt angle of a laser beam is slightly altered compared to the tilt angle of the other beams.[19] This means that laser beams not ideally adjusted relative to the vertical, lead to a substrate potential with phasonic jags which density is usually orientation dependent. In Fig. 7a we plot the tiling of the whole system shown partially in Fig. 5g. One can clearly notice the alignment of two large domains along two main directions.

In Fig. 7b we show a cut of the underlying interference pattern. The transparent white lines highlight some characteristic lines and show the existence of jags along certain directions. These phasonic jags can be better identified by means of Fourier filtering.[19] In fact, one of the signatures of a phasonic jags is the appearance of anisotropic shifts in the positions of Bragg peaks in the diffraction pattern (not shown here). Fig. 7c,d,e show the back Fourier transform of the shifted peaks along three directions. The resulting intensity distribution images proof that the density of the jaggs is the smallest for the two directions along which the bands are aligned.

Conclusion

In conclusion, we have presented an investigation of the structural phase transition of triangular crystals interacting with a decagonal light pattern. Our experiments show that the transformation from a triangular crystalline structure to a decagonal quasiperiodic phase undergoes a two stage process. First, bands of square tiles are formed leading to a destruction of the local periodic ordering perpendicular to the bands. For higher laser intensities, pentagonal tiles form, reflecting the decagonal quasiperiodic ordering. We also investigate in detail, how an Archimedean like tiling phase gradually develops from a triangular crystal. Here, the length of bands with square tiles increases with laser intensity. Finally, we demonstrated that the orientation of bands, in particular in the Archimedean like tiling phase is highly correlated to the presence of phasonic strain fields.

Acknowledgements

We acknowledge Michael Schmiedeberg and Holger Stark for helpful discussions. This work is financially supported by the Deutsche Forschungsgemeinschaft (BE 1788/5).

References

1 D. Shechtman, I. Blech, D. Gratias and J. W. Cahn, *Phys. Rev. Lett.*, 1984, **53**, 1951 1953.
2 D. Levine and P. J. Steinhardt, *Phys. Rev. Lett.*, 1984, **53**, 2477.
3 A. P. Tsai, J. Q. Guo, E. Abe, H. Takakura and T. J. Sato, *Nature*, 2000, **408**, 537 538.
4 L. Bindi, P. J. Steinhardt, N. Yao and P. J. Lu, *Science*, 2009, **324**, 1306 1309.
5 T. Dotera and T. Gemma, *Philos. Mag.*, 2006, **86**, 1085 1091.
6 X. B. Zeng, G. Ungar, Y. S. Liu, V. Percec, S. E. Dulcey and J. K. Hobbs, *Nature*, 2004, **428**, 157 160.
7 D. V. Talapin, E. V. Shevchenko, M. I. Bodnarchuk, X. Ye, J. Chen and C. B. Murray, 2009, 461, pp. 964 967.
8 J. M. Dubois, *J. Phys.: Condens. Matter*, 2001, **13**, 7753 7762.
9 J. Y. Park, D. F. Ogletree, M. Salmeron, R. A. Ribeiro, P. C. Canfield, C. J. Jenks and P. A. Thiel, *Science*, 2005, **309**, 1354 1356.
10 M. E. Zoorob, M. D. B. Charlton, G. J. Parker, J. J. Baumberg and M. C. Netti, *Nature*, 2000, **404**, 740 743.
11 J. Ledieu, L. Leung, L. H. Wearing, R. McGrath, T. A. Lograsso, D. Wu and V. Fournee, *Phys. Rev. B: Condens. Matter Mater. Phys.*, 2008, **77**, 073409.
12 K. J. Franke, H. R. Sharma, W. Theis, P. Gille, P. Ebert and K. H. Rieder, *Phys. Rev. Lett.*, 2002, **89**, 156104.
13 H. R. Sharma, M. Shimoda, A. R. Ross, T. A. Lograsso and A. P. Tsai, *Phys. Rev. B: Condens. Matter Mater. Phys.*, 2005, **72**, 045428.
14 J. Ledieu, J. T. Hoeft, D. E. Reid, J. A. Smerdon, R. D. Diehl, N. Ferralis, T. A. Lograsso, A. R. Ross and R. McGrath, *Phys. Rev. B: Condens. Matter Mater. Phys.*, 2005, **72**, 035420.
15 V. Fournée, T. C. Cai, A. R. Ross, T. A. Lograsso, J. W. Evans and P. A. Thiel, *Phys. Rev. B: Condens. Matter Mater. Phys.*, 2003, **67**, 033406.
16 J. Mikhael, J. Roth, L. Helden and C. Bechinger, *Nature*, 2008, **454**, 501 504.
17 M. Schmiedeberg, J. Roth and H. Stark, *Phys. Rev. Lett.*, 2006, **97**, 158304.
18 J. Mikhael, M. Schmiedeberg, S. Rausch, J. Roth, H. Stark and C. Bechinger, *Proc. Natl. Acad. Sci. U. S. A.*, 2010, **107**, 7214 7218.
19 M. Schmiedeberg, J. Mikhael, S. Rausch, J. Roth, L. Helden, C. Bechinger and H. Stark, *Eur. Phys. J. E*, 2010, **32**, 25 34.
20 C. Gutsche, U. F. Keyser, K. Kegler and F. Kremer, *Phys. Rev. E: Stat., Nonlinear, Soft Matter Phys.*, 2007, **76**, 031403.
21 Y. L. Han, Y. Shokef, A. M. Alsayed, P. Yunker, T. C. Lubensky and A. G. Yodh, *Nature*, 2008, **456**, 898 903.
22 M. M. Burns, J. M. Fournier and J. A. Golovchenko, *Science*, 1990, **249**, 749 754.
23 S. P. Gorkhali, J. Qi and G. P. Crawford, *J. Opt. Soc. Am. B*, 2006, **23**, 149 158.
24 M. A. Glaser and N. A. Clark, in *Advances in Chemical Physics*, ed. S. A. R. I. Prigogine, John Wiley and Sons, Inc., New York City, 1993, pp. 543 709.
25 P. J. Steinhardt and H. C. Jeong, *Nature*, 1996, **382**, 431 433.
26 M. Schmiedeberg and H. Stark, *Phys. Rev. Lett.*, 2008, **101**, 218302.
27 S. C. Glotzer and A. S. Keys, *Nature*, 2008, **454**, 420 421.
28 B. Freedman, R. Lifshitz, J. W. Fleischer and M. Segev, *Nat. Mater.*, 2007, **6**, 776 781.
29 E. Abe, S. J. Pennycook and A. P. Tsai, *Nature*, 2003, **421**, 347 350.